TREATMENT OF ORGANIC POLLUTANT IN WASTEWATER BY USING CERIUM OXIDE NANOPARTICLES

Goutam Mandal[1]*, Baibaswata Bhattacharjee[2]

Abstract

In this report, we fabricate spherical cerium oxide (CeO_2) nanoparticles by simple wet chemical method. Utilizing X-ray diffraction (XRD), the crystallinity was investigated. Hexagonal structure of the unit cell was found in the XRD study. The morphology of the fabricated nanoparticles was investigated using Field emission Scanning Electron Microscope (FESEM). Optical band gap was calculated by using UV-Vis spectra. The partial/complete mineralization of organic dye can be utilized using semiconductor nano-photocatalyst. Here, photocatalytic activity of the fabricated CeO_2 was explored by the degradation of methylene blue (MB) dye using visible light irradiation. Different operational parameters e.g. initial dye concentration, catalyst doses and pH and their effect on photodegradation was also studied.

Keywords: Cerium oxide (CeO_2), Photocatalysis, Photocatalytic degradation, Safranin-O, Methylene blue (MB).

[1]*Department of Physics, Bankura Zilla Saradamani Mahila Mahavidyapith, Bankura- 722101, India
[1]*Department of Physics, Bankura University, Bankura – 722 146, West Bengal, India
[1]Email: phy.gmandal@gmail.com
[2]Department of Physics, Ramananda College, Bishnupur, Bankura – 722 122, West Bengal, India

***Corresponding Author:** Goutam Mandal
*Department of Physics, Bankura Zilla Saradamani Mahila Mahavidyapith, Bankura- 722101, India
*Department of Physics, Bankura University, Bankura – 722 146, West Bengal, India
Email: phy.gmandal@gmail.com

DOI: 10.48047/ecb/2023.12.si6.576

1. Introduction

Wastewaters from textile, paper, medicine and some other industries contains residual dyes and water contaminants, those are not easily degradable [1]. Dyes are amongst the major water pollutants generally present in effluents of textile, leather, paper, printing, cosmetics, petroleum, plastic, food, paint, rubber, and pharmaceutical industries [2]. Additionally, water polluted with dyes can be a potential threat to aquatic life [3]. Several treatment technologies such as adsorption [4-5], oxidation [6], biological treatment [7], coagulation and flocculation [8], membrane processes [9], chlorination [10], ozonation [11], etc. can be used for treatment of wastewater containing dye pollutants. However, due to their complex structure, dyes are very difficult to decolorize using the available techniques [12]. These process however only transfer dyes from liquid to solid phase and further treatment required for secondary pollutant [13]. The use of semiconductor nano-photocatalyst gives the benefit of lower cost, higher efficiency and also suitable recycling [14-15]. As a result, a number of progressive oxidation techniques have been used industrially to speed up the oxidation of refractory contaminants by producing extremely reactive hydroxyl radicals ($^{\cdot}OH$) [16-17].

Nanoscale cerium oxide (CeO_2) is a wide and direct band gap (3.19 eV) semiconductor [18]. In nanoscale CeO_2 shows tuning band gap and optical properties. They are good candidate for catalytic applications due to their larger exciton binding energy[19-20] . In fact, CeO_2 is one of the most studied catalytic materials, with several examples of its use in accelerating various organic processes in the literature, including carbon monoxide oxidation, catalytic incineration of aromatic hydrocarbons, and mineralization (ozonation) of aniline. Several researchers have reported on CeO_2's photocatalytic activity [21] and its capacity to degrade synthetic dyes more efficiently than titanium oxide.

2.Materials and methods

Materials

Cerium nitrate hexahydrate [$Ce(NO_3)_3 .6H_2O$] and potassium carbonate [K_2CO_3] with purity ≥99.5% were purchased from Sigmae Aldrich and used as received. Methylene Blue (MB) as a model pollutant from textile industry was obtained from SRL, India. In the photodegradation experiment, a stock solution of MB (1.0 g/L) was used and

diluted to the required concentration with deionized water. All chemical reagents were of analytical grade and used as received. Samples were then preserved in the desiccators over anhydrous $CaCl_2$ for further use.

2.1. Synthesis CeO_2 nanoparticles

We adopted the conventional wet chemical methods to synthesize zinc oxide nanoparticles (NPs) at room temperature. To synthesize CeO_2 NPs, at first in a beaker 0.05M,100mL solution of Cerium nitrate was prepared by dissolving Ce $(NO_3)_3$.$6H_2O$ in distilled water. Similarly, 0.03M, 100mL solution of potassium carbonate (K_2CO_3) was prepared by dissolving K_2CO_3 in distilled water. Aqueous solution of potassium carbonate (50 mL) was added drop by drop with cerium nitrate under constant stirring about 15 h at room temperature. A white precipitate of cerium (III) carbonate was seen in the mixed solution. The precipitation was collected using filter paper and washed with distilled water several times. Resulting precipitation dried in a hot air oven at 60ºC for 3 h, followed by calcination at 600ºC for 6 h to form the crystalline pure phase.

2.2. Instrumentation

X-ray diffraction (XRD) data were collected in a Rigaku X-ray diffractometer using Cu-Kα radiation with the wavelength of 1.54 Å over an angular selection of $20°<2\theta<80°$. Optical absorption measurements were accomplished using a Systronics AU 2703 double beam UV-Visible spectrophotometer with a wavelength range of 200-800 nm. At 5 kV accelerating voltages, the surface morphology of the catalysts was investigated using a ZEISS field emission scanning electron microscope (FESEM). The elemental distribution of ZnO was investigated using energy-dispersive X-ray spectroscopy (EDX) on a Leo1430VP microscope with a 5 kV operating voltage.

2.3. Photocatalytic dye degradation experiments

In a cylindrical pyrex-glass cell of 10 cm in height, aqueous solutions containing the photocatalyst were used to degrade methylene blue by photocatalysis. [22]. The suspensions were irradiated under atmospheric condition with white light. The suspension was sampled out at regular intervals during the irradiation. The dispersion was magnetically stirred for 30 minutes (in the dark) prior to illumination to establish adsorption equilibrium between the photocatalyst surface and the methylene blue dye. As a result, the effect of surface adsorption on methylene blue removal is eliminated. The influence of the pH of the initial solution was evaluated at pHs ranging from 2 to 11 (adjusted using HCl (0.1M) and NaOH (0.1 M)), while methylene blue dye concentration was preset at 30 mg/L of photocatalyst. Photocatalyst dosage was varied from 0.1 to 1 g/L, for 30 mg/L of methylene blue solution, at pH 7. The effect of methylene blue dye concentration was also investigated by adjusting it from 10 mg/L to 80 mg/L at a constant pH of 7 in the presence of 0.7 g/L photocatalyst. Each sample was taken out at regular intervals and rapidly centrifuged at 15,000 rpm for 10 minutes to remove any suspended photocatalysts for analysis. Finally, a UV visible spectrophotometer was used to measure the absorbance of methylene blue in the supernatant liquid at the maximum adsorption wavelength of methylene blue, λ_{max}= 660 nm.

The degradation rate (D) of the dye was calculated using Eq. (1):

$$D\% = (A_0 - A_t/A_0) \times 100 \text{ …….. (1)}$$

where A_0 represents the initial absorbance of methylene blue solution (blank),
and A_t its absorbance after t min of irradiation/ reaction.
According to the Beer-Lambert's law A_0 and A_t are proportional to C_0 and C_t,
where C_t and C_t are the concentration of blank and sample at (t) time.

The photodegradation rate constant (k, min^{-1}) was calculated from the slope of the straight-line segment of the plot of $\ln\left(\frac{C_t}{C_0}\right)$ vs. t as a function of the used experimental parameters. The photodegradation of pollutants follows the pseudo first-order kinetics according to the Langmuir-Hinshelwood model [23-24], so the photo decolorization rate of each sample was studied using Eq. (2):

$$\ln\left(\frac{C_t}{C_0}\right) = kt \text{……(2)}$$

The optical properties of the photocatalysts were studied by UV visible absorption spectroscopy at room temperature.

3. Results and discussion

3.1. Absorption Spectrum

The amount of the energy band gap of CeO_2 NPs was estimated by analysing their optical characteristics using UV visible spectroscopy. The

band gap energy s was calculated depending on the absorption spectrum of the sample according to the following Eq. (3):

$$E_g = \frac{1240}{\lambda_g} \quad \text{.....(3)}$$

Where, $E_g$is the optical band gap energy of the photocatalyst, λ_g is the wavelength in nm used as the absorption edge.

The optical absorption is studied with in wavelength range 200nm to 1000 nm. The observed optical absorption spectrum for the variation of optical absorbance of the grown CeO_2 NPs dispersed in water is shown in Fig. 1(A). The maximum absorbance peak was seen at ≈ 352 nm. The optical absorption coefficient (α) has been calculated from the Lambert law in the wavelength region 200–900 nm. The optical band gap (Eg) of the as-arranged nanoparticles have been figured utilizing the Tauc equation [25]:

$$(\alpha h\upsilon)^{\frac{1}{n}} = B(h\upsilon - E_g) \quad \text{.....(4)}$$

Where $\alpha$is the absorption coefficient, h is Planck's constant and υ is the frequency ($\upsilon = \frac{c}{\lambda}$, λ is the wavelength, c is the light speed). For the allowed direct band gap, the value of n equal to 1/2. Exponent n depends on the category of transition and it may have values 1/2, 2, 3/2 and 3 corresponding to the allowed direct, allowed indirect, forbidden direct and forbidden indirect transitions, respectively [26]. B is a constant and generally called band tailing parameter. Thus, the band gap energy was obtained graphically from $(\alpha h\upsilon)^2$ vs. hυ for direct transition, extrapolating the linear part on the abscissa according to Eq. (4). According to this method, the band gap of the samples can be approximated as shown in Fig. 1(B). The estimated direct band gap is 3.52 eV.

Wavelength reliance of optical absorption property of semiconductor can be communicated by the following Eq. (5) [27]:

$$\alpha = \alpha_0 \exp(^{h\upsilon}/_{E_U}) \quad \text{.....(5)}$$

By plotting ln(α) with the incident photon energy hγ, the Urbach energy E_U can be resolved. The variation of ln(α) with the incident photon energy hγ appeared in Fig. 1(C). Urbach energy is acquired from the inverse of the incline (see Fig. 1(C)). The calculated value of the Urbach energy is 1.026 eV.

3.2. Scanning electron microscope (SEM) analysis

The surface morphology, size, shape and growth mechanism of CeO_2 nanoparticles were investigated through SEM analysis (Fig. 1(D)). These SEM images display closely packed nearly spherical and randomly oriented nanoparticles. There appears some enhancement in the porosity and reduction in the density due to liberation of gases which created surface pores and holes as obvious from these images.

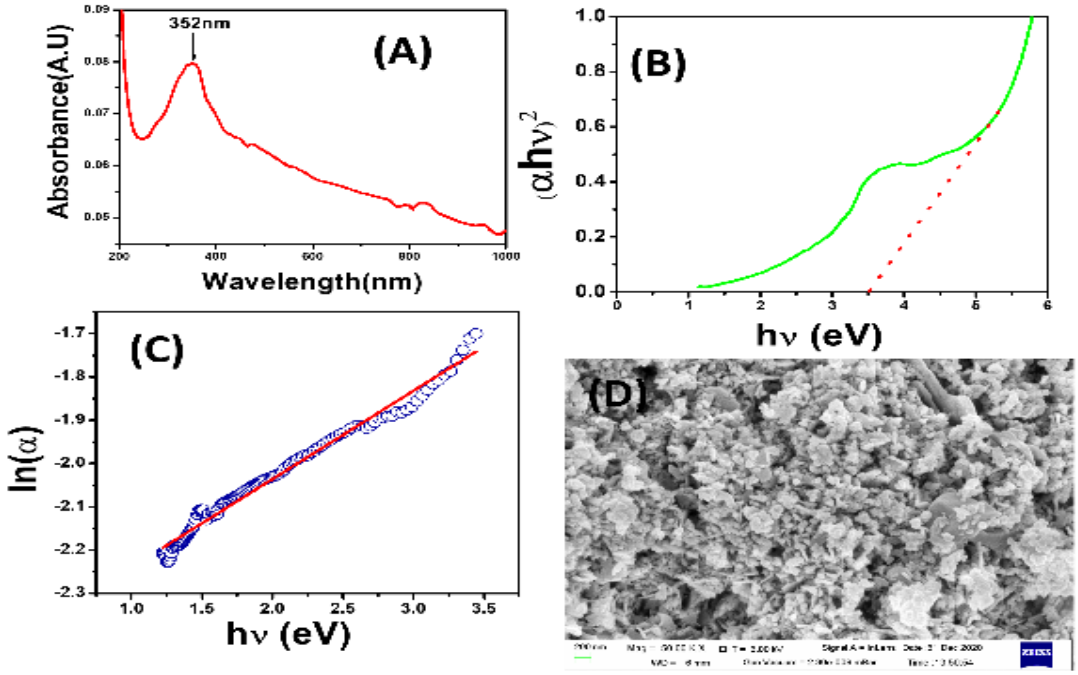

Fig. 1-(A) UV-VIS spectrum of CeO_2 NPs, (B) Tauc's plot for bandgap determination, (C) Plot of ln(α) vs. photon energy (hυ), (D) FESEM image of CeO_2 NPs

3.3. X ray diffraction

The XRD pattern shown in Fig. 2(A) shows that the unit cell of the synthesized CeO_2 nano-crystal is cubic with the presence of the peaks (111), (200), (220), (311), (222), (400), (331), and (420) [28]. The nanoparticle size is calculated from the Scherrer formula [29]:

$$D = \frac{K\lambda}{\beta cos\theta} \ldots\ldots\ldots\ldots\ldots\ldots (6)$$

Here, D is the crystalline size and K = 0.94, for copper radiation. The average particle size from this equation is found to be ~ 32.73 nm. The strain (ε) and grain size (D) of the nanomaterial is also calculated using the Williamson-Hall (W-H) equation [30]:

$$\beta cos\theta = \frac{K\lambda}{D} + 4\varepsilon sin\theta \ldots\ldots\ldots\ldots\ldots\ldots (7)$$

The average size (D) and dislocation density $d = \frac{1}{D^2}$ are calculated [31]. The average crystal size of CeO_2 NPs is found to be 37.88 nm from the Scherrer formula and 32.73 nm from the fitted result of the W-H equation (Fig. 2(B)). The value of strain is 0.0014 from the fitted result of the W-H equation and 0.0052 from Scherrer equation. The value of dislocation density is 3.127 × 10^{-3} /nm^2 from the result of the W-H and 1.928 × 10^{-3} /nm^2 from the Scherrer equation.

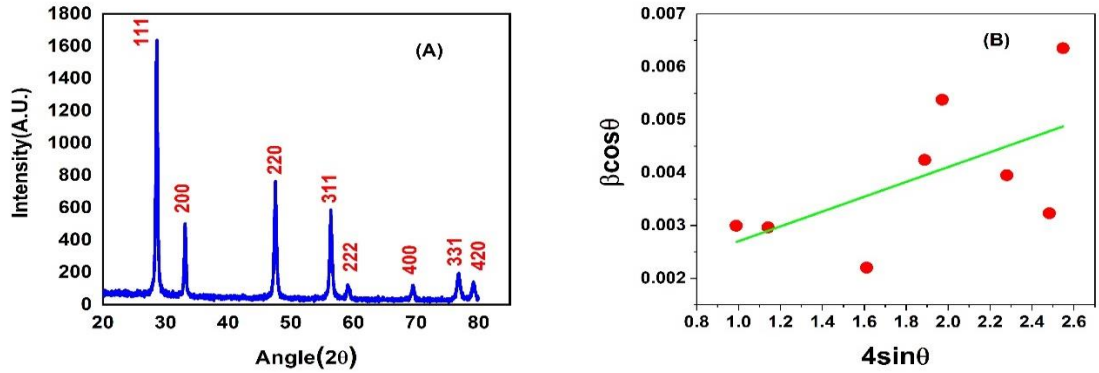

Fig. 2-(A) XRD of CeO_2 NPs, (B) plot of $\beta cos\theta$ vs $sin\theta$

3.4. Effect of operating parameters on the photocatalytic degradation of MB

3.4.1. Effect of catalyst dosage

The rate of photodegradation of a chemical pollutant was found to be a function of photo catalytic dosage in heterogeneous photo catalysis [32-33]. In present work, photo catalyst dosage was varied from 0.1 to 1 g/L, for 30 mg/L of methylene blue solution, at pH 7.

The photocatalytic degradation rates increased as the catalyst load increased. With 0.1 g/L catalyst, the percentage degradation was found to be 38%. When the catalyst load was raised to 0.2 g/L and 0.5 g/L, the percentage was 46% and 59%, respectively, whilst a catalyst load of 0.7 g/L resulted in nearly 87% degradation after 60-70 minutes. Any increase in catalyst load more than 0.7 g/L resulted in poor degradation as shown in Fig. 3(D).

The above observations can be attributed to the availability of active sites on the catalyst surface and the penetration of light into the solution. With increasing catalyst loading, the increased turbidity blocks the light transmission into the solution. The phenomenon is reported in the literature as "scattering" or "screening" effect [32-38].

The degradation can be explained as follows:

When photon energy E> E_g [band gap energy] then electrons (e−) in conduction band and holes (h+) in valance band are generated. The photo-generated holes could either directly oxidize the dye or react with hydroxyl (OH−) or H_2O to generate hydroxyl radicals (·OH). The photoelectrons reduce oxygen (O_2) adsorbed on the photocatalyst surface into superoxide radical (·O_2 −). Finally, dye was decomposed by the generated ·OH and O^-_2. The reaction is given below:

$$CeO_2 + h\nu \longrightarrow CeO_2 (h^+ + e^-)$$

$$h^+ + OH^- \text{ or } H_2O \longrightarrow OH$$

$$e^- + O_2 \longrightarrow O^-_2$$

$$OH^- / \cdot O^-_2 + \text{dye} \longrightarrow CO_2 + H_2O + \text{inorganic molecules}$$

Based on the above observations, 0.7g/L was selected as an optimum catalyst load for further experiments. The photodegradation of MB dye

with catalyst concentration 0.7g/L is shown in Fig. 3(A) and the plot of $\frac{C_t}{C_0}$ vs time is shown in Fig. 3(B). The rate constant saw calculated from Fig. 3(C) and was found 0.035 min^{-1}.

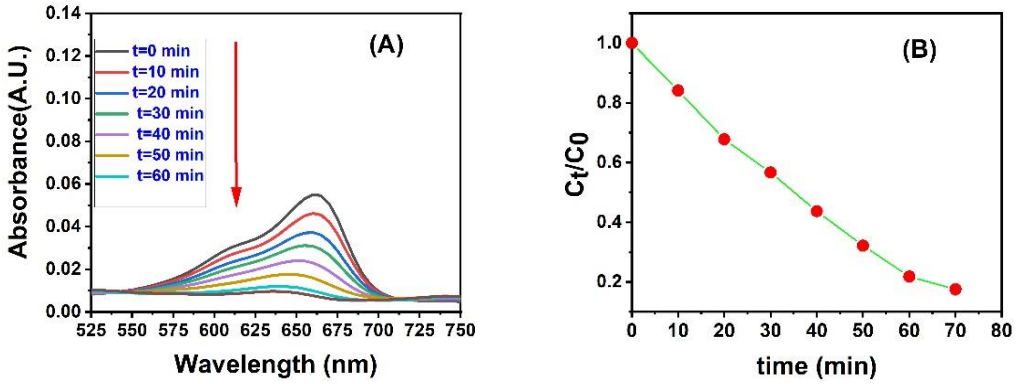

Fig. 3-(A) photo degradation of MB dye with dose 0.7g/L (B) plot of $\frac{C_t}{C_0}$ vs time

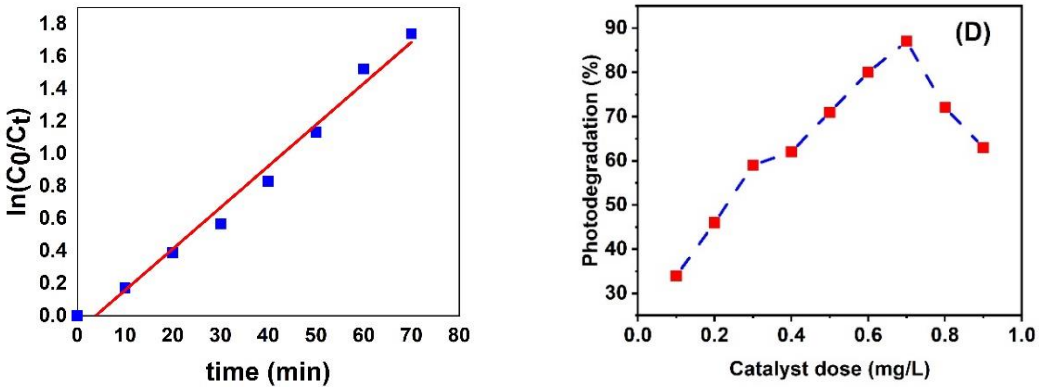

Fig. 3- (C) Photocatalytic degradation kinetic curves (D) Effect of catalyst loading on photocatalytic degradation of MB dye

3.4.2. Effect of initial dye concentration

Initial dye concentration is an indirect measure of opacity. In this study, the effect of initial dye concentration in the range of 10mg/L to 50mg/L was studied at optimum catalyst loading of 0.7 g/L. The results are shown in Fig. 3(E). The variation in the initial dye concentration was selected based on reported in the literature for degradation of various other dyes [39-41]. It is observed that the % dye remaining in the solution increases with increase in the initial dye concentration. For the concentration of 10mg/L, nearly 95% degradation was observed within 60–70 min. However, at an initial dye concentration of 20mg/L, 30mg/L, 40mg/L, 50mg/L the % dye degradation was observed to be 63% and 35%, 26% and 11% respectively. The above observations clearly indicate that photo catalysis reactions are very sensitive to the initial dye concentration.

A comparable pattern has been observed previously in the photodegradation of azo dyes such as Eosin Yellow [42] and Sunset Yellow [43]. The phenomenon is attributed to the formation of ·OH radicals and their probability to react with dye molecules. When the parameters such as catalyst loading and light intensity are constant, the amount of free radicals generated remains constant. Therefore, at higher initial dye concentrations, an insufficient amount of radicals to target the large amount of dye molecules results in poor degradation.

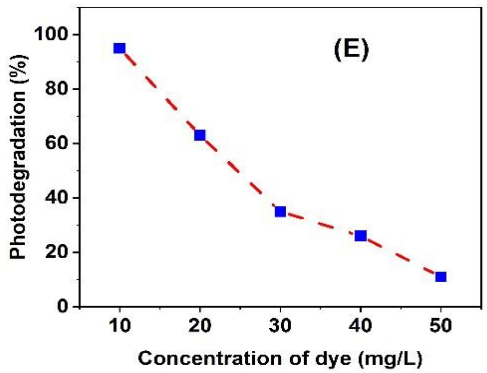

Fig. 3-(E) Effect of dosage on the properties of CeO_2 photocatalysts (F)

3.4.2. Effect of pH

The effect of solution pH in the range of 2–11 on the photocatalytic degradation of 10mg/L MB dye at an optimum catalyst loading of 0.7 g/L was studied. It was seen that at a solution pH of 2, the % degradation of the dye was 85%. Whereas, a nearly complete dye degradation was observed with the solution pH of 3. Increasing the pH value from 3 to 6 (which is natural pH of the solution), did not improved the degradation and the results were comparable to those obtained with pH of 3. At a higher solution pH of 11, the % dye degradation significantly decreased. It is believed that changing the pH of the reaction solution changes the adsorption of the target compound on the surface of the catalyst. The adsorption is expected to be maximum around the isoelectric point (IEP) of the catalyst [44].

4. Conclusion

The present study investigates the potential of chemically synthesized CeO_2 for photocatalytic degradation of methylene blue dye. Complete degradation of the 10mg/L dye solution was achieved within 60 min with 0.7 g/L synthesized CeO_2, natural pH of the solution and at room temperature. The catalyst showed better photocatalytic activity compared to combustion synthesized and commercial catalysts at same reaction conditions. Thus, CeO_2 nanoparticles can be used for waste water treatment and for better environment.

Acknowledgement

Authors are thankful to the Department of Physics, Bankura University and Bankura Zilla Saradamani Mahila Mahavidyapith.

References

1. Seth, Prahlad K. "Chemical contaminants in water and associated health hazards." Water and Health (2014): 375-384.
2. Husain, Qayyum. "Peroxidase mediated decolorization and remediation of wastewater containing industrial dyes: a review." Reviews in Environmental Science and Bio/ Technology 9 (2010): 117-140.
3. Kadirvelu, Kavipriya, et al. "Utilization of various agricultural wastes for activated carbon preparation and application for the removal of dyes and metal ions from aqueous solutions. " Bioresource technology 87.1(2003):129-132.
4. Crini, Gregorio. "Non-conventional low-cost adsorbents for dye removal: a review." Bio resource technology 97.9 (2006): 1061-1085.
5. Bhatnagar, Amit, and A. K. Jain. "A comparative adsorption study with different industrial wastes as adsorbents for the removal of cationic dyes from water." Journal of Colloid and Interface Science 281.1 (2005): 49-55.
6. Kang, Shyh-Fang, Chih-Hsiang Liao, and Shei-Tue Po. "Decolorization of textile wastewater by photo-Fenton oxidation technology." Chemosphere 41.8 (2000): 1287-1294.
7. Dos Santos, André B., Francisco J. Cervantes, and Jules B. Van Lier. "Review paper on current technologies for decolourisation of textile wastewaters: perspectives for anaerobic biotechnology." Bioresource technology 98.12 (2007): 2369-2385.
8. Choi, Jeong-Hak, et al. "Application of synthetic polyamine flocculants for dye wastewater treatment." Separation Science and technology 36.13 (2001): 2945-2958.
9. Chen, Dingwang, and Ajay K. Ray. "Photo catalytic kinetics of phenol and its derivatives over UV irradiated TiO2." Applied Catalysis B: Environmental 23.2-3 (1999): 143-157.
10. Daneshvar, Nezamaddin, Darioush Salari, and A. R. Khataee. "Photocatalytic degradation of azo dye acid red 14 in water on ZnO as an alternative catalyst to TiO2." Journal of photochemistry and photobiology A: chemistry 162.2-3 (2004): 317-322.
11. Pouretedal, H. R., and A. Kadkhodaie. "Synthetic CeO2 nanoparticle catalysis of methylene blue photodegradation: kinetics and mechanism." Chinese Journal of Catalysis 31.11-12 (2010): 1328-1334.
12. Augugliaro, Vincenzo, et al. "Photocatalytic oxidation of cyanides in aqueous titanium dioxide suspensions." Journal of catalysis 166.2 (1997): 272-283.
13. Tanaka, Keiichi, Kanjana Padermpole, and Teruaki Hisanaga. "Photocatalytic degradation of commercial azo dyes." Water research 34.1 (2000): 327-333.
14. Xiao, Jianliang, et al. "L-cysteine-reduced graphene oxide/poly (vinyl alcohol) ultralight aerogel as a broad-spectrum adsorbent for anionic and cationic dyes." Journal of Materials Science 52 (2017): 5807-5821.
15. Parmar, Kaushal R., et al. "Synthesis of acetone reduced graphene oxide/Fe 3 O 4 composite through simple and efficient chemical reduction of exfoliated graphene oxide for removal of dye from aqueous solution." Journal of Materials Science 49 (2014): 6772-6783.
16. Wang, Wanqiang, et al. "Template- free Fabrication of ZnS/TiO2 Photocatalyst with

Macrochannels." Journal of the Chinese Chemical Society 65.2 (2018): 252-258.
17. Kiwaan, Hala A., et al. "Efficient photo catalytic degradation of Acid Red 57 using synthesized ZnO nanowires." Journal of the Chinese Chemical Society 66.1 (2019): 89-98.
18. Carter, Daniel C., et al. "Preliminary crystallographic studies of four crystal forms of serum albumin." European Journal of Biochemistry 226.3 (1994): 1049-1052.
19. Renuka, N. K., A. K. Praveen, and C. U. Aniz. "Ceria rhombic microplates: Synthesis, characterization and catalytic activity." Microporous and mesoporous materials 169 (2013): 35-41.
20. Zhai, Yongqing, Shaoyang Zhang, and Hui Pang. "Preparation, characterization and photocatalytic activity of CeO2 nanocrystalline using ammonium bicarbonate as precipitant. " Materials Letters 61.8-9 (2007): 1863-1866.
21. Piriyanon, Jirayus, et al. "Fabrication of MoS 2/Ag 3 PO 4 S-scheme photocatalyst for visible-light-active degradation of organic dye and antibiotic in wastewater." Journal of Materials Science: Materials in Electronics 32 (2021): 19798-19819.
22. Kiwaan, Hala A., et al. "Efficient photocatalytic degradation of Acid Red 57 using synthesized ZnO nanowires." Journal of the Chinese Chemical Society 66.1 (2019): 89-98.
23. Moradi, Banafsheh, Gholamreza Nabiyouni, and Davood Ghanbari. "Rapid photo-degradation of toxic dye pollutants: green synthesis of mono-disperse Fe 3 O 4–CeO 2 nanocomposites in the presence of lemon extract." Journal of Materials Science: Materials in Electronics 29 (2018): 11065-11080.
24. Zinatloo-Ajabshir, Sahar, Sobhan Mortazavi-Derazkola, and Masoud Salavati-Niasari. "Preparation, characterization and photo catalytic degradation of methyl violet pollutant of holmium oxide nanostructures prepared through a facile precipitation method." Journal of Molecular Liquids 231 (2017): 306-313.
25. Tauc, J., Radu Grigorovici, and Anina Vancu. "Optical properties and electronic structure of amorphous germanium." physica status solidi (b) 15.2 (1966): 627-637.
26. Essawy, Amr A. "Silver imprinted zinc oxide nanoparticles: Green synthetic approach, characterization and efficient sunlight-induced photocatalytic water detoxification." Journal of Cleaner Production 183 (2018): 1011-1020.
27. Bhattacharjee, B., et al. "Synthesis and optical characterization of sol–gel derived zinc sulphide nanoparticles confined in amorphous silica thin films." Materials Chemistry and Physics 78.2 (2003): 372-379.
28. Tambat, Sneha, Sanjivani Umale, and Sharad Sontakke. "Photocatalytic degradation of Milling Yellow dye using sol–gel synthesized CeO2." Materials Research Bulletin 76 (2016): 466-472.
29. Patterson, A. L. "The Scherrer formula for X-ray particle size determination." Physical review 56.10 (1939): 978.
30. Kahouli, M., et al. "Structural and optical properties of ZnO nanoparticles prepared by direct precipitation method." Superlattices and Microstructures 85 (2015): 7-23.
31. Dini, G., et al. "Flow stress analysis of TWIP steel via the XRD measurement of dislocation density." Materials Science and Engineering: A 527.10-11 (2010): 2759-2763.
32. Sivalingam, G., et al. "Photocatalytic degradation of various dyes by combustion synthesized nano anatase TiO2." Applied Catalysis B: Environmental 45.1 (2003): 23-38.
33. Chen, Dingwang, and Ajay K. Ray. "Photocatalytic kinetics of phenol and its derivatives over UV irradiated TiO2." Applied Catalysis B: Environmental 23.2-3 (1999): 143-157.
34. Daneshvar, Nezamaddin, Darioush Salari, and A. R. Khataee. "Photocatalytic degradation of azo dye acid red 14 in water on ZnO as an alternative catalyst to TiO2." Journal of photochemistry and photobiology A: chemistry 162.2-3 (2004): 317-322.
35. Pouretedal, H. R., and A. Kadkhodaie. "Synthetic CeO2 nanoparticle catalysis of methylene blue photodegradation: kinetics and mechanism." Chinese Journal of Catalysis 31. 11-12 (2010): 1328-1334.
36. Augugliaro, Vincenzo, et al. "Photocatalytic oxidation of cyanides in aqueous titanium dioxide suspensions." Journal of catalysis 166.2 (1997): 272-283.
37. Sontakke, Sharad, Jayant Modak, and Giridhar Madras. "Photocatalytic inactivation of Escherischia coli and Pichia pastoris with combustion synthesized titanium dioxide." Chemical engineering journal 165.1 (2010): 225-233.
38. Benabbou, A. K., et al. "Photocatalytic inactivation of Escherischia coli: Effect of concentration of TiO2 and microorganism, nature, and intensity of UV irradiation.

"Applied Catalysis B: Environmental 76.3-4 (2007): 257-263.
39. Mozia, Sylwia, Maria Tomaszewska, and Antoni W. Morawski. "Photocatalytic degradation of azo-dye Acid Red 18. " Desalination 185.1-3 (2005): 449-456.
40. Grzechulska, Joanna, and Antoni Waldemar Morawski. "Photocatalytic decomposition of azo-dye acid black 1 in water over modified titanium dioxide." Applied Catalysis B: Environmental 36.1 (2002): 45-51.
41. Daneshvar, Nezamaddin, Darioush Salari, and A. R. Khataee. "Photocatalytic degradation of azo dye acid red 14 in water on ZnO as an alternative catalyst to TiO2." Journal of photochemistry and photobiology A: chemistry 162.2-3 (2004): 317-322.
42. Debnath, Sushanta, et al. "Optimization and mechanism elucidation of the catalytic photo-degradation of the dyes Eosin Yellow (EY) and Naphthol blue black (NBB) by a polyaniline-coated titanium dioxide nanocomposite. " Applied Catalysis B: Environmental 163 (2015): 330-342.
43. Rajamanickam, D., P. Dhatshanamurthi, and M. Shanthi. "Enhanced photocatalytic efficiency of NiS/TiO2 composite catalysts using sunset yellow, an azo dye under day light illumination." Materials Research Bulletin 61 (2015): 439-447.
44. Bhatkhande, Dhananjay S., Vishwas G. Pangarkar, and Anthony A. C. M. Beenackers. "Photocatalytic degradation for environmental applications–a review." Journal of Chemical Technology & Biotechnology: International Research in Process, Environmental & Clean Technology 77.1 (2002): 102-116.